

# Incorporating User Utility in a Smart Microgrid with Distributed Generation and Elastic Demand

Benjamin Brooks  
Asset Integrity & Performance  
DNV GL-Energy  
Bristol, UK  
Email: Ben.Brooks@dnvgl.com

Jing Jiang, Hongjian Sun  
School of Engineering and Computing Sciences  
Durham University  
Durham DH1 3LE, UK  
Email: {Jing.Jiang, Hongjian.Sun}@durham.ac.uk

**Abstract**— Demand Side Management (DSM) will play a large role in creating a pathway to a low carbon future. Microgrids are an ideal test bed for DSM within the Smart Grid (SG) framework, allowing for increased integration of distributed generation (DG), here focused on distributed Renewable Energy Sources (RESs). Existing work uses conservative estimates to model the stochastic nature of RESs, resulting in inaccuracies in simulation results. Large uncertainty in user specific participation in DSM programs exists. This paper develops a flexible energy load function, effectively incorporating different user’s behaviour patterns into the DSM framework. Uncertainty in connecting small-scale wind generation into the smart microgrid is reduced by using an expected cost function to accurately map predicted wind speed to power output. Actual wind speed is varied across numerous sub-horizons within each time slot by using a pseudo-random number generator. The stochastic nature of renewable generation is effectively managed, producing a robust simulation. Model sensitivities are investigated and graphical results presented.

**Keywords**— Demand side management; microgrid; smart grid; distributed renewables; user utility function

## I. INTRODUCTION

The smart grid, as the transformed electricity grid, fitted with modern electronics and upgraded control systems, provides more information and better communication between electricity suppliers and users of the grid [1][2]. The upgrade from traditional electricity grid to smart grid will enable consumers to actively participate in electricity trading and wholesale price auctions from the demand side. Demand side management (DSM) or demand response (DR) techniques are at the very heart of the smart grid [3]. With DSM, the end-use customers change their electric usage from their normal consumption patterns in response to changes in the price of electricity over time; DSM thus facilitates more efficient use of current generation capacity. As well as facilitating a two-way flow of information, the smart grid also supports two-way flow of electricity, thus paving the way for demand-side generation (distributed generation (DG)) and integration. These generators can be driven by conventional sources but will most likely be renewable energy sources (RES) such as wind turbines or solar photovoltaic (PV) units.

To limit the uncertainty that distributed generators can have on the future grid there is a strong consensus that DG and DSM should be implemented within microgrids. A microgrid is a

networked group of distributed energy sources located at the distribution network side and can provide energy to small geographical areas [4]. The network of microgrid intends to operate in a grid-connected mode, or to be intentionally islanded or isolated from the grid bus. Microgrids are an ideal test bed for DSM within the SG framework, allowing for increased integration of DG, here focused on distributed RESs.

A review of the electricity market in the smart grid environment from the demand-side was undertaken in [3]. Notable pilot projects of DSM have been established; For example in [5], Enexis, a Dutch distribution system operator, pioneered a project gleaning field data to inform research and evaluate washing machine load potential for smart grid integration. In [4], game-theoretic methods are employed to enable cooperative energy exchange using a cooperative game. It is also shown that a non-cooperative game can accurately model the interactions between loads and sources in a microgrid. A novel load control strategy for use in a microgrid in islanded mode has been developed in [6] for use in a community reliant on legacy infrastructure or for the clusters of microgrids that will precede the full implementation of the smart grid. Parallel load schedule optimisation for distributed generators is explored in [7]. An autonomous scheme ensures high levels of grid security and retains privacy as the load profiles of individual users are not disclosed. Distributed economic dispatch and DSM for a microgrid operating in grid-connected mode with high RES penetration is explored in [8]. An optimal scheduling strategy is proposed to address the uncertainty arising from the stochastic nature of RES; But the approach proposed in [8] didn’t incorporate knowledge of the physical power mappings of a wind turbine for a given wind speed. Different from previous work, this paper incorporates the real characteristics of DGs and public electricity use. In this paper, we offer a direct link between natural power (wind) and electrical generation. In addition, this paper develops a novel utility varying model that is proven to be more representative of the general public. Uncertainty associated with RESs and the subjective nature of consumer energy choices are incorporated in the model. A flexible energy load function is proposed to effectively incorporate different user’s behaviour patterns into the DSM framework.

The rest of this paper is organized as follows. Section II specifies the demand model, distributed generator model, and the conventional generator model. The microgrid energy

management optimisation is analyzed in Section III. Simulation results are shown in Section IV; Section V concludes the paper.

## II. MODEL DESCRIPTION

Consider a microgrid with  $n$  energy loads,  $m$  conventional generators and  $r$  distributed RES. The simulation period is broken down into 8 distinct timeframes, each representing a one-hour period of time. Using a microgrid enables optimisation of collective generators and loads, rather than optimising for each individual user.

### A. Demand Model

Loads in a household environment can generally be broken down into 3 distinct types: fixed, energy and schedulable.

#### 1) Fixed Demand

This is the load required within any given time horizon to satisfy basic user needs, e.g., refrigerators and lighting as detailed in [7]. Here this load is represented by a fixed value for a given time period, as this load cannot physically be shifted by the load controller. This is representative of a real system as for a given dark period in the day there is a minimum amount of light required by an individual living in the developed world. This fixed load is denoted as  $D^f$ .

#### 2) Energy Load Demand

Energy loads, denoted as  $D_n$ , where  $n \in \{1, \dots, N\}$ , have power consumption  $P'_{Dn} \in [P'^{min}_{Dn}, P'^{max}_{Dn}]$ . This type of load can be adjusted by users or by the centralised energy management system in response to a contract or agreement with the user. However, a reduction in this type of load incurs a decline in consumer utility, here defined as the satisfaction derived per kWh of electricity consumed. Examples of these dispatchable loads include heating in winter or air conditioning in summer. As suggested in [9], we use a cost utility function incorporating an additional  $\theta$  term (normalised to  $0 \leq \theta \leq 1$ ) to scale the function in order to sort different customer usage behaviours. Here, a quadratic function is chosen to numerically model the amount of utility  $U(\theta, P'_{Dn})$  that can be derived from a given energy load  $D_n$  in time period  $t$ . The general Taylor series expansion of the function is

$$U(\theta, P'_{Dn}) = u_0 + u_1\theta + u_2(P'_{Dn}) + \frac{u_3(P'_{Dn})^2}{2} + u_4(P'_{Dn})\theta + \frac{u_5\theta^2}{2}. \quad (1)$$

At zero load, the cost to the user should also be nil, thus  $u_0 = 0$ . Here, users are ranked from most willing ( $\theta = 0$ ) to least willing ( $\theta = 1$ ). In addition, the function  $U(\theta, P'_{Dn})$  must satisfy the following three conditions

$$\frac{\partial}{\partial \theta} \left( \frac{\partial U}{\partial P'_{Dn}} \right) < 0, \quad \frac{\partial U}{\partial P'_{Dn}} \geq 0, \quad \frac{\partial^2 U}{\partial (P'_{Dn})^2} < 0. \quad (2)$$

The first condition is because that a quadratic function must satisfy the sorting condition and the users are sorted from most willing to least willing to shed load. This implies that the rate of change of the cost gradient should be always decreasing within the limits for  $\theta$ . The function should be non-decreasing in  $P'_{Dn}$  as increasing load brings increased cost, giving the

second condition. In addition, the cost function must be concave as it is assumed that as the customer increases their load the rate of change in marginal benefit is assumed to be decreasing (i.e., each additional kWh of electricity doesn't linearly increase user satisfaction), which gives the third condition. Using these constraints, we have

$$U(\theta, P'_{Dn}) = K_1(P'_{Dn})^2 + K_2P'_{Dn} - K_2P'_{Dn}\theta, \quad (3)$$

where  $K_1 = 0.5u_3 < 0$ ,  $K_2 = u_2 > 0$ ,  $-K_2 = u_4 < 0$ .

#### 3) Schedulable Load Demand

This type of load has a total energy requirement over a given timeframe, and must remain within power consumption limits, both maximum and minimum. Examples include washing machines and dishwashers. This class of load is omitted from this paper as the technology and cost of these devices is currently prohibitive for large-scale deployment.

### B. Distributed Generator (RES) Model

Here, a small wind turbine (such as the Norwin 200kW turbine) is used to model a distributed generator in the microgrid.  $P'_{Rr}$  is the power consumption from RES unit  $r$  at a given time  $t \in T = \{1, 2, \dots, T\}$ . To further model the time variant nature of the wind due to local pressure gradients, each time horizon  $T$  is divided into 8 further sub-horizons  $i \in I = \{1, \dots, I\}$ . For each time horizon  $T$  there is a maximum value for the wind speed, below which the sub-horizon wind speed values are permitted to vary in a quasi-random fashion dictated by a Mersenne Twister pseudorandom number generator. These real-time wind speeds are contained within the 8 ( $T = 8$ ) by 8 ( $I = 8$ ) matrix  $\{\mathbf{V}\}$ .

The relationship between the mechanical power output  $W^t$  in Watts, and the wind speed  $v$  in m/s is given by

$$W^t = c_p(\lambda, \beta) \frac{\rho A}{2} v^3, \quad (4)$$

where  $c_p(\lambda, \beta)$  denotes the coefficient of performance of the wind turbine in terms of tip speed ratio (of the blade tip to free stream wind velocity)  $\lambda$  [10], and blade pitch angle  $\beta$ ;  $\rho$  is the air density in  $\text{kg/m}^3$ ; and  $A$  is the turbine swept area in  $\text{m}^2$ . The generic equation for  $c_p$  is detailed in [10], using an induced tip speed ratio to effectively model the behaviour of a real turbine. The maximum possible performance coefficient ( $c_p$ ) for this turbine is 0.48, well below the Betz limit of 0.5928. Here the mechanical output power is assumed to be converted through a direct-drive synchronous generator using a power converter with an electrical efficiency of 0.95.

The decision variable for the RES is  $P'_{Rr}$  which is the total scheduled power transfer for RES unit  $r$  in time horizon  $t$ . As the power mapping for the wind speed is known, the discrepancy between the known power output of a turbine ( $W^t$ ) at each time horizon is denoted as  $[P'_{Rr} - W^t]^+$  when there is a shortage of production or  $[P'_{Rr} - W^t]^-$  when there is a surplus of production. A feature of the microgrid is that it can trade electricity with the main grid (in grid-connected mode) in the event of a surplus or shortage of generation. The shortfall in electricity is bought at a known purchase price  $\alpha^t$ , while the surplus electricity is sold at a known selling price  $\beta^t$ . As such

an expected cost function  $F$  (expected value due to stochastic nature of wind speed  $v$  denoted in (5) as  $\mathbf{E}$ ) is developed,

$$F(\{P_R^t\}) = \mathbf{E} \left( \sum_{t=1}^T \alpha^t [P_R^t - \sum_{i=1}^I W_i^t(v_i^t)]^+ - \beta^t [P_R^t - \sum_{i=1}^I W_i^t(v_i^t)]^- \right), \quad (5)$$

where  $P_R^t$  collects the scheduled power consumption decision variables for time  $t$  and  $F$  is the objective function. By including the real power mappings the inherent conservatism in more stochastic and probabilistic estimates can be bypassed, ensuring a more representative and reliable optimisation model.

### C. Conventional Generator Model

Inevitably the uncertainty associated with wind energy leads microgrid owners or stakeholders to invest in or upgrade conventional DG. The model provides scope to employ a carbon penalty feature to heap additional cost on to fossil fuel fired conventional generation.  $P_{Gm}^t$  represents the power produced by the  $m$ th conventional generator. This relationship is given by an increasing convex function  $C(P_{Gm}^t)$ , as the cost of running the generator increases in a quadratic fashion for increasing output as described in [11]

$$C(P_{Gm}^t) = z \cdot (g_0 + b(P_{Gm}^t) + c(P_{Gm}^t)^2),$$

subject to  $\frac{\partial C}{\partial (P_{Gm}^t)} \geq 0$  and  $\frac{\partial^2 C}{\partial (P_{Gm}^t)^2} \geq 0$ . (6)

This function is developed in the same fashion as previously shown for the utility function, but using different coefficients ( $g_0$ ,  $b$  and  $c$ ) and a multiplier  $z$  representing the fuel cost in £/MJ. The two conditions ensure that the function is increasing and the convexity condition.

## III. MICROGRID ENERGY MANAGEMENT OPTIMISATION

### A. Optimisation Model

The optimisation approach in this paper targets all three decision variables detailed in section III: conventional generation  $P_{Gm}^t$ , elastic energy loads  $P_{Dn}^t$  and renewable energy scheduling  $P_{Rr}^t$  are all input into the model. The objective function incorporates the sum across multiple time horizons and multiple generation and demand sources. The problem essentially amounts to minimising the net social cost within the microgrid for its users and stakeholders. That is minimising the cost of conventional generation, and the expected cost of volatile RES minus the utility of the energy load.

$$\min_{\{P_{Gm}^t, P_{Dn}^t, P_{Rr}^t\}} \sum_{t=1}^T \left( \sum_{m=1}^M C_{Gm}^t(P_{Gm}^t) + F(\{P_R^t\}) - \sum_{n=1}^N U_{Dn}^t \right), \quad (7)$$

subject to:

$$P_{Gm}^{\min} \leq P_{Gm}^t \leq P_{Gm}^{\max}, m \in M, t \in T, \quad (7a)$$

$$P_{Dn}^{\min} \leq P_{Dn}^t \leq P_{Dn}^{\max}, n \in N, t \in T, \quad (7b)$$

$$P_R^{\min} \leq P_R^t \leq P_R^{\max}, \forall t \in T, \quad (7c)$$

$$\sum_{m=1}^M (P_{Gm}^{\max} - P_{Gm}^t) \geq S^t, \forall t \in T, \quad (7d)$$

$$\sum_{m=1}^M P_{Gm}^t + P_R^t - \sum_{n=1}^N P_{Dn}^t = D^t, \forall t \in T. \quad (7e)$$

Constraints (7.a), (7.b) and (7.c) all relate to the maximum and minimum bounds for each parameter. These are the physical limits giving a minimum output or consumption for a generator or load. Constraint (7.d) indicates the spinning reserve  $S^t$  that must be maintained in the system across all timeframes. This is a fixed value and represents the need for a generation reserve to compensate for any generators outages or line faults that may occur in the microgrid. Finally constraint (7.e) is the load balance equation, simply ensuring that all demand in the system is met by supply. At any one time within the grid the consumption has to equal the production.

It is important to note here that the electricity selling price  $\alpha^t$  must be lower than the purchase price  $\beta^t$  for all  $t \in T$ . Clearly microgrid generation cannot directly compete with large scale national generators to sell electricity at the Market Clearing Price (MCP), thus as a direct corollary the purchase price in a real physical system will always be higher than the selling price of a small-scale distributed generator. Indeed EDF Energy offers a flexible Power Purchase Agreement (PPA) named ‘clarity’ [12], to suppliers generating over 250MW a year. Assuming an arbitrary load factor of 20% for a distributed wind turbine, this would indicate installing a 150kW turbine to qualify for this PPA, assuming a downtime for maintenance of <5% of total annual operational time.

This corollary ensures convexity in the solution, as the RES function  $F(\{P_R^t\})$ , can be shown to depend on the operations of non-negative weighted summation and pointwise maximum (over an infinite set) [8], which preserve convexity.

### B. Use of fmincon and Linear Programming

The Matlab® solver fmincon has been used in this project to optimise the objective function around 3 separate decision variable divisions. The solver attempts to find a constrained minimum of a linear or nonlinear, multivariable function.

The choice of a suitable starting point for the optimisation is essential to building a robust and flexible algorithm. Constraints (7a-7e) are all linear constraints. A simple Linear Program operation is run within these linear constraints for a zero value objective function of appropriate dimension to give an initial estimate for the optimisation. By using the simplex method in this fashion to provide initial conditions for the solver, enables the optimisation to reliably and efficiently produce results. A range of diagnostic tools is subsequently used to analyse and present the project findings.

The solving of the RES function was non-trivial. A ‘NOT’ function was employed to clearly separate the surplus and shortage generation conditions, evaluate these as separable functions and then combine them again for summation in the objective function.

#### IV. NUMERICAL SIMULATIONS AND DISCUSSION

For the test environment, the microgrid was chosen to consist of  $M = 2$  conventional generators,  $N = 2$  flexible energy loads and  $R = 1$ , a single RES generator (using the previously detailed wind power mapping function). The maximum and minimum bounds for each of these functions are shown in Table I below.

TABLE I. LOWER & UPPER BOUNDS OF DECISION VARIABLES

	$P_{G1}$	$P_{G2}$	$P_{D1}$	$P_{D2}$	$P_R$
Min (kWh)	10	8	5	8	0
Max (kWh)	50	45	35	40	35

Shown in Table II are the fixed, base loads that must be served at all times, regardless of the price of electricity. These values have been chosen to reflect the average power curve of daily UK demand [13] but scaled down to a microgrid sized demand. The lower and upper bounds for the five ( $M+N+R$ ) decision variables shown above have been carefully chosen to ensure that the respective functions are strictly increasing and either convex or concave depending on the nature of the parameter. The conventional generator cost function is given as  $C(P_{Gm}^t) = 0.4P_{Gm}^2 + 40P_{Gm}$ . The utility cost function is given as  $U(P_{Dn}^t) = -0.6P_{Dn}^2 + 60P_{Dn} - 60\theta P_{Dn}$ . This function is not immediately convex, and thus would prohibit the objective function from reaching a local minimum. As the utility function is subtracted from the other cost functions in the objective function this lack of convexity is restored, leading to an inherently solvable problem.

TABLE II. DEMAND OF FIXED LOAD

Time	1	2	3	4	5	6	7	8
$D^t$ (kWh)	25	30	45	58	70	67	50	42

Fig. 1 shows the base case in grid-connected mode, modelling users with typically inelastic attitudes to load reduction. Wind velocity varies between a maximum level of 18m/s ( $\approx 35$  knots) and a minimum of 0m/s. Selling prices ( $\beta^t$ ) for renewable generation are relatively high, thereby favouring surplus generation and export to the grid. As expected the scheduled output from the RES unit is at a maximum value of 35kWh for 3 out of the 8 timeframes above, showing an inclination of the algorithm to profit from the perhaps over generous selling prices, here straying to within 1.5p/kWh of the purchase price at times. The utility function can be seen to be perhaps less influential than expected, as the load is at a minimum level for the majority of the timeframes. This would be indicative of a user that will continually adjust their usage to increase utility. For example this type of user is happy to pay slightly more to have a warm house than to save the money involved. Thus this user clearly has a low  $\theta$  value (here in fact this is zero). The optimisation approach functions correctly, taking on average less than 10 seconds using a quad core 2.3GHz processor.

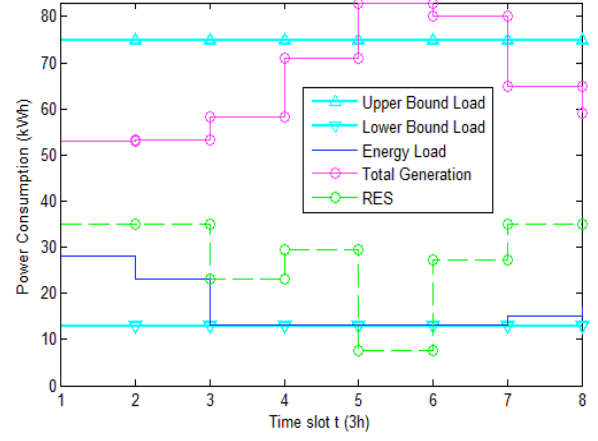


Fig. 1. Optimal power schedule base case

#### A. Objective Function Sensitivity Analysis

The purpose of this section is to analyse the effect of changing the model parameters to determine its sensitivity to fluctuations in objective function coefficients and input values. Informed comment on the robustness of the optimisation approach can then subsequently be made.

First the coefficients of the conventional generators are varied. The default value is initially set as  $C_{Gm}^t = 0.4P_{Gm}^2 + 40P_{Gm}$ . If the linear coefficient term is reduced by 12.5% to a value of 35, a noticeable increase is observed in the scheduled amount of energy load across the board, most significant in time slots 3 and 7 where increases of up to 5kWh are observed. This indicates high sensitivity to price volatility of conventional generation within this microgrid. If for example the conventional generator is a diesel fired installation, fluctuations in the price of diesel would have a direct impact on the users' behaviour. Users would increase their consumption in line with cheaper fuel prices, and thus increase the utility derived from their use. Indeed varying the fuel cost multiplier  $z$  has a similar effect on the optimisation.

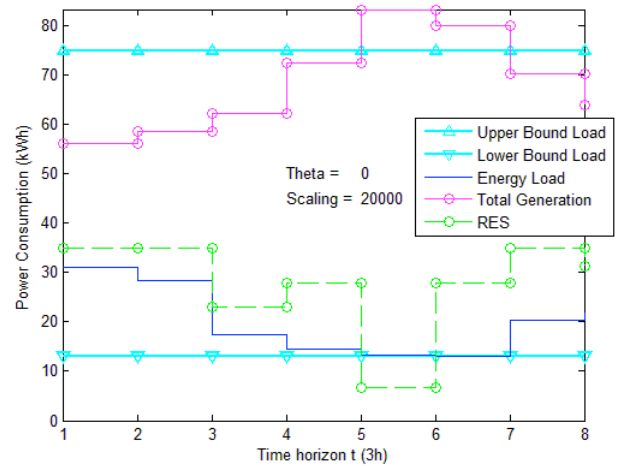


Fig. 2. Noticeable increases in committed energy load across multiple time horizons for a reduction in the linear coefficient of the cost function of conventional generators

The utility function sensitivity is investigated by first adjusting the  $K_2$  coefficient in the model i.e., the scaling factor of the  $x$  term and the  $x^\theta$  term in the utility cost function. Ensuring consistency with previous analysis, the  $K_2$  coefficient sees an increase of 12.5% (i.e.  $K_2$  changes from 60 to 67.5). As a result noticeable increases in conventional generation and energy load are observed as shown in Fig. 3. Time slot 5 seems to be somewhat of an anomaly here. This is due to inherent uncertainty built in to the model as well as the non-linearity of the wind turbine wind-speed-to-power-output mapping function  $W_t$ . In time slot 5 the maximum allowable wind speed is set at 16m/s, higher than in time slot 4 where the wind blows at a maximum of 14m/s. Due to the pseudorandom number generator used here the actual wind speed incident on the turbine across all 8 time sub-horizons has a maximum value of 11m/s, with time-varying average of just 4.75m/s.

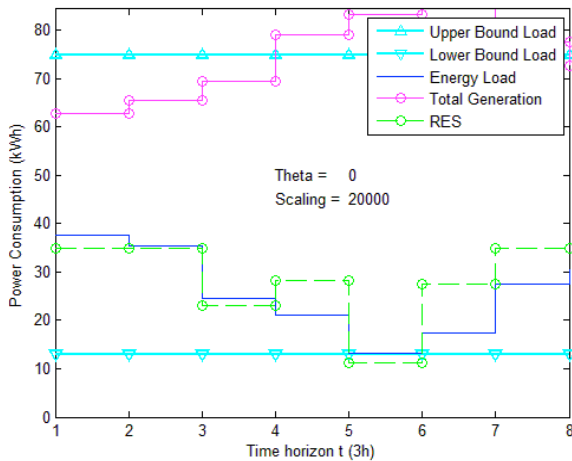


Fig. 3. Increases as a result of an adjustment of the utility function

The non-linear form of the function  $W_t$  reflects the real energy conversion efficiency characteristics of a wind turbine, i.e. for wind speeds approaching turbine rated wind speed the power output is proportionally higher. Also, the fixed load requirement peaks during this time period to 70kWh. Thus to remain within the constraints of generation whilst maintaining spinning reserve, the optimisation drives energy load consumption to the lower rail in spite of the considerable magnitude of the resultant diminished utility.

### B. Variation of $\theta$ to demonstrate flexibility for different users

The  $\theta$  term in the utility function is used to scale output in terms of consumers' willingness to consume additional electricity to increase utility. Fig. 4 shows the change in energy load utility due to a change in the value of  $\theta$  between a minimum of 0 (representing consumers who derive high satisfaction for a unit increase in load), and a maximum of 1 (exhibits no elasticity in demand, saves money at all costs). This effectively ranks the users predilection to adjust their load for a given cost. The users with lower values for  $\theta$  are those most inclined to reduce or increase their load, these users would include young families, those classed as 'fuel poor' (where  $>10\%$  income spent on energy) and other users who exhibit high elasticity in demand. The users with larger values

for  $\theta$  are those in need of high electricity during the day, for example the elderly, hospitals, and small industry who cannot curtail load at a given time.

Fig. 4 demonstrates the effect on the RES generation and load within the microgrid for a range of consumer electricity consumption attitudes,  $\theta$ , in period 1. The relative change in energy loads and renewable generation is quantified using the cumulative difference between the decision variable magnitudes after each iteration of the algorithm. The absolute value is taken for clarity of presentation. Thus with increasing  $\theta$  on the x-axis the relative change in the optimisation decision variables is displayed on the y-axis, indicating that the discrete change in  $\theta$  from 0 to 1 effectively tiers the users as expected. Low cumulative difference magnitude indicates that the user is inclined to increase their load in period 1 for low  $\theta$  values. Those users with  $\theta$  values above 0.5 show little inclination to change their consumption.

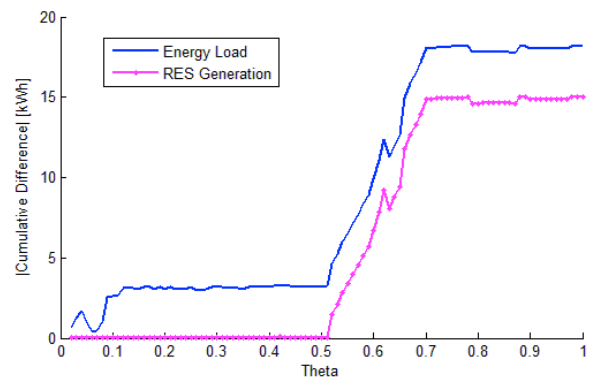


Fig. 4. Effect on generation and demand when varying  $\theta$  (theta) from 0 to 0.8, in time period 1

### C. RES Purchase & Selling Price

The purchase and selling prices for the RES unit has a marked effect on the model. The previous tests detailed have been for a relatively high selling price when compared to the purchase price. The model proves to be relatively insensitive to changes in the purchase price.

TABLE III. RES FUNCTION DETAILS: PURCHASE AND SELLING PRICES AND WIND VELOCITY

Time	1	2	3	4	5	6	7	8
$\alpha^t$ (£/kWh)	15	20	57	65	80	77	50	45
$\beta^t$ (£/kWh)	13.5	18	51.3	58.5	72	69.3	45	40.5
$v$ (m/s)	1	10	12	14	16	18	14	5

When the  $\beta^t$  value is reduced to values of less than 10 £/kWh across all time slots, the effect on the model is relatively low. This is due to the magnitude of the RES function being relatively low in comparison to the other terms in the objective function. The cost of purchasing energy from the main grid is not prohibitive across all timeframes, even in the event of large shortfalls between scheduled power and actual production in the event of low wind speeds. The maximum wind speed values are given in Table III above with actual wind speed

varying across the 8 sub-horizons below this maximum. Thus a shortage occurs in time slots 1, 2 and 8.

The RES function reflects the base load and varies accordingly. Fig. 5 shows the effect of varying purchase and selling prices on the elasticity of the model. It is shown that the model is far less sensitive to selling price fluctuation when compared to changes in purchase price (just under 34.5 times more for RES generation curves as shown in Fig. 5). For unit increases in purchase prices of  $>32\text{£/kWh}$  when compared to values in Table III, it is clearly uneconomical to purchase from the grid and the optimisation converges to schedule RES solely for when there is enough wind to support a pure export of electricity to the main grid. The enlarged subplot of Fig. 8 shows small fluctuations in energy load for a unit increase in selling price greater than  $65\text{£/kWh}$ .

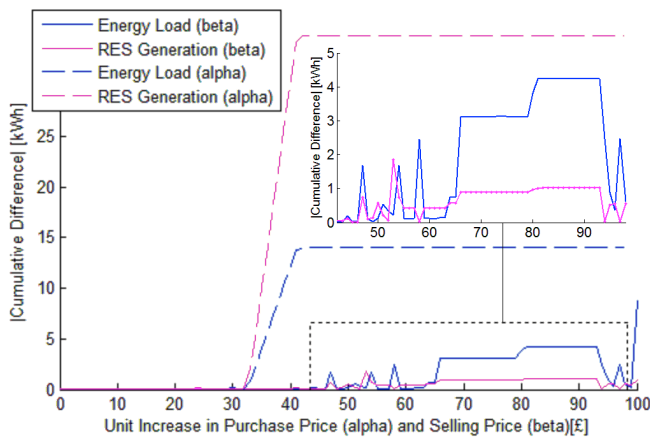


Fig. 5. Effect on energy loads and RES generation in time period 1 when i) selling price is increased for fixed purchase price (dashed lines) and ii) purchase price is increased for fixed selling price (solid lines)

## V. CONCLUSION

DSM techniques as discussed in this paper help reduce consumer costs and  $\text{CO}_2$  emissions by facilitating more efficient use of current generation capacity. Reducing the peak-to-average demand ratio using techniques presented in this paper has the potential to reduce the cost to electricity consumers. In this paper, we consider smart microgrids for DSM with distributed generation, and have developed a novel utility varying model through adapting the RES and user utility functions to make the simulation more representative of a physical microgrid. Uncertainty associated with RESs and the subjective nature of consumer energy choices have been incorporated in the model. It is shown that by using a Taylor series expansion of a generic two-variable quadratic function, a flexible and tailored user utility/satisfaction function can be realised. This function is easily adaptable to reflect a particular user or group of users' predisposition to adjust their consumption in relation to an incentive. In addition, it is known that electricity does not behave as a normal economic quantity but rather shows large inelasticity in the demand curve. The user utility function proposed in this paper goes some way to incorporating this inelasticity into the objective function.

Results show that the presented model successfully incorporates RES into the microgrid environment. Direct power mapping for a given wind speed accurately predicts the electrical power output for a given time horizon. By using a bounded Mersenne Twister random number generator for targeted sub-horizons, the stochastic nature of the wind is captured within the simulation. This paper bypasses the conservatism of a worst-case transaction cost, giving a more representative estimate of overall wind power output.

## ACKNOWLEDGMENT

This work was supported by the European Commissions Horizon 2020 Framework Programme (H2020/2014-2020) under Grant Agreement 646470, SmarterEMC2 Project.).

## REFERENCES

- [1] W. Y. Chiu, H. Sun, and H. V. Poor, "A Multiobjective Approach to Multimicrogrid System Design," *IEEE Trans. Smart Grid*, vol. 6, no. 5, pp. 2263-72, Sept 2015.
- [2] J. Jiang, H. Sun and W. Y. Chiu, "Energy efficient massive MIMO system design for smart grid communications," 2016 IEEE International Conference on Communications Workshops, Kuala Lumpur, pp. 337-341, 2016.
- [3] X. Fang, "Smart Grid - The New and Improved Power Grid - A Survey," *IEEE Communications Surveys and Tutorials*, vol. 14, no.4, pp. 962-966, Dec 2012.
- [4] W. Saad, Z. Han, H. V. Poor and T. Basar, "Game-Theoretic Methods for the Smart Grid: An Overview of Microgrid Systems, Demand-Side Management, and Smart Grid Communications," *IEEE Signal Processing Magazine*, vol. 29, no. 5, pp. 86-105, Sept. 2012.
- [5] E. Klaassen, C. Kobus, M. van Huijkelom, J. Frunt and H. Slootweg, "Evaluation of washing machine load potential for smart grid integration," in 48th International Universities Power Engineering Conference (UPEC), Dublin, 2013, pp. 1-6.
- [6] T. Vandoorn, B. Renders, L. Degroote, B. Meersman and L. Vandevelde, "Active Load Control in Islanded Microgrids Based on the Grid Voltage," *IEEE Transactions on Smart Grid*, vol. 2, no. 1, pp. 139-151, 2011.
- [7] P. Yang, P. Chavali, E. Gilboa and A. Nehorai, "Parallel Load Schedule Optimization with Renewable Distributed Generators in Smart Grids," *IEEE Transactions on Smart Grid*, vol.4, no.3, pp. 1431-1441, 2013.
- [8] Y. Zhang, N. Gatsis and G. B. Giannakis, "Robust Energy Management for Microgrids with High-Penetration Renewables," *IEEE Transactions on Sustainable Energy*, vol. 4, no. 4, pp. 944-953, 2013.
- [9] M. Fahrioglu and F. L. Alvarado, "Using Utility Information to Calibrate Customer Demand Management Behavior Models," *IEEE Transaction on Power Systems*, vol. 16, no. 2, pp. 317 - 322, 2001.
- [10] S. Rahman and M. Pipattanasomporn, "Modeling and Simulation of a Distributed Generation-Integrated Intelligent Microgrid," Department of Defense Strategic Environmental Research and Development Program (SERDP), Blacksburg, 2010.
- [11] D. Kirschen and G. Strbac, *Fundamentals of Power System Economics*, Chichester: Wiley-Blackwell, 2004
- [12] EDF Energy. Simple Power Purchase Agreements for new generators. London, 2013. [Online]. Available: <http://www.edfenergy.com/products-services/large-business/sell-generate-energy/assets/pdf/B2B-FS-Clarity-Power-Purchase-Agreement-001-1113.pdf>
- [13] J. Palmer, N. Terry and T. Kane, *Early Findings: Demand side management*. Cambridge Architectural Research Limited, Element Energy and Loughborough University. June 2013. [Online]. Available: [http://www.chpa.co.uk/medialibrary/2013/06/21/9f3a86f6/early\\_finding\\_s.pdf](http://www.chpa.co.uk/medialibrary/2013/06/21/9f3a86f6/early_finding_s.pdf).